

Effect of orbital symmetry on high-order harmonic generation from molecules

Bing Shan, Shambhu Ghimire, and Zenghu Chang*

J. R. Macdonald Laboratory, Department of Physics, Kansas State University, Manhattan, Kansas 66506, USA

(Received 24 June 2003; published 27 February 2004)

It was found experimentally with increasing the laser ellipticity that the intensity of the 45th order harmonic from O₂ decreases slower than that from N₂. The difference is attributed to the fact that the recombination probability is suppressed for O₂ but enhanced for N₂ in a linearly polarized field. Simulation results obtained by extending the Lewenstein model to molecules agreed qualitatively with the experimental discoveries.

DOI: 10.1103/PhysRevA.69.021404

PACS number(s): 42.50.Hz, 33.80.Rv

High order harmonic generation (HHG) from atoms and molecules exposed to a strong laser field is an interesting subject for its potential applications as a coherent ultrafast x-ray source [1–3]. Compared to the study of harmonic generation from atoms, few efforts have been devoted to molecules. On one hand, early experiments showed harmonic generation from molecules is similar to that from atoms [4,5]. On the other hand, it was found theoretically that molecules (or molecular ions) are attractive candidates for harmonic generation because of their two (or more)-center structure [6,7]. Recently, it was discovered experimentally that the cutoff order of high harmonic generation from O₂ molecules is much higher than that from Xe atoms though their ionization potentials are very close [8], which is related to the ionization suppression of O₂ molecules [9–11]. Under elliptically polarized field, the recollision electron is driven away by the transverse field component from its parent ion so that the harmonic yield drops quickly with increasing the driving field ellipticity [5,12]. This property could be employed to produce attosecond pulses with polarization gating [13,14]. For such applications, it is interesting to know whether harmonic generation from some molecules is more susceptible to ellipticity than that from atoms. Flettner *et al.* compared the harmonic generation for N₂ and Ar gases and reported that the harmonic yield from N₂ drops slower than that from Ar with increasing the driving field ellipticity [15]. In this communication, the dependence of high order harmonic generation yield on the ellipticity of the driving laser field for O₂ and N₂ was compared experimentally for the first time.

The experiments were carried out at the *Kansas Light Source* laser facility. The one-stage amplifier system outputs 4 mJ, 25 fs pulses at a center wavelength of 790 nm. Part of the laser output is led to a high-order harmonic generation system, which is composed of a gas nozzle, a grazing incidence mirror, a transmission grating, an MCP intensifier, and a CCD camera [16]. The gas nozzle has an outlet diameter of 75 μm and the gas density in the interaction region was $\sim 5 \times 10^{17}$ molecules/cm³. The ellipticity of the laser was adjusted by a combination of a half waveplate and a quarter waveplate. In the experiment, we set the optic axis of the quarter waveplate along the dispersion direction of the transmission grating. The ellipticity was changed by rotating the

half waveplate so that the major axis of the elliptical polarization does not change. By doing this, the effect of the polarization dependent diffraction efficiency of the grating is minimized.

Firstly, the scaling of the cutoff with the laser intensity for molecules was compared with that for atoms. The laser power is changed by a half waveplate/polarizer combination before the pulse compressor of the laser. The cutoff of the harmonic spectrum is defined as the highest detectable harmonic order. The measured relationships between cutoff energy and laser intensity are shown in Fig. 1. The slope of the linear part is the same for atoms and for molecules, i.e., they all follow the scaling law of the recollision mechanism [17,18]. The results indicate that under our experimental condition, the harmonic signal is from the recollision channel, instead of other possible mechanisms proposed by [7] that have different scaling laws. In Fig. 1(b) the cutoff from O₂ is much higher than that from Xe at the saturation intensities; such a cutoff extension is due to ionization suppression as reported earlier [8].

Figure 2(a) shows the ellipticity dependence of 21st order HHG for Ar and N₂ gases. In this measurement, the 25 fs, 1.5 mJ laser pulses were focused by a lens with an 800-mm focal length. The on target intensity was $\sim 2.3 \times 10^{14}$ W/cm². The signal from Ar gas was normalized to that from N₂, so as to make them unity for linear polarization. The same normalizations were done in Figs. 3 and 4 for the clarity of presentation. In the measurement, the signal/noise ratio $(I_{\text{signal}} - I_{\text{background}})/(I_{\text{signal}} + I_{\text{background}})$ is larger than 30% over 4 orders of magnitude (the range above

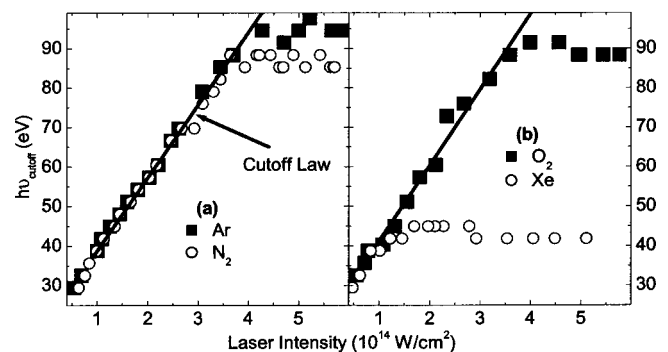


FIG. 1. Measured HHG cutoff with respect to the laser intensity for two pairs of atomic and molecular gases with similar ionization potential and different orbital symmetry. (a) Ar vs N₂; (b) Xe vs O₂.

*Email address: chang@phys.ksu.edu.

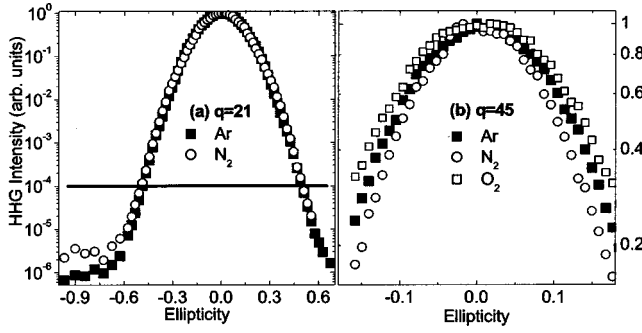


FIG. 2. (a) Measured ellipticity dependence of 21st HHG of Ar and N₂ gases. The laser intensity is 2.3×10^{14} W/cm². The region above the horizontal line has a signal/noise ratio $(I_{\text{signal}} - I_{\text{background}})/(I_{\text{signal}} + I_{\text{background}})$ better than 30%; (b) measured ellipticity dependence for the 45th order harmonic from N₂, O₂ and Ar gases. The laser intensity is 3.5×10^{14} W/cm².

the horizontal line in the figure). The 21st order intensity dependence on ellipticity for these two gases was the same over five orders of magnitude. The results are different from the previous results reported by Flettner *et al.* [15]. They found that the harmonic yield from N₂ drops slower than that from Ar with increasing the driving field ellipticity. It seems to us that the slower drop of harmonic signal for N₂ in [15] arose from the contribution of the detector background.

Figure 2(b) shows the 45th order harmonic signal dependence on the laser ellipticity for O₂, N₂ and Ar gases. The laser pulse energy was 2.8 mJ and the beam was focused by a 500 mm focal length lens. The intensity was $\sim 3.5 \times 10^{14}$ W/cm². In the measurement, we used 0.2 μ m Al+0.2 μ m parylene (C₈H₈) filters. The transmission of this filter set increases from less than 10% at 50 eV to $\sim 60\%$ at 70 eV. So the low order unwanted signal and fundamental laser were suppressed to obtain a better signal/noise ratio at the 45th order harmonic (~ 70 eV). Because the signal at this

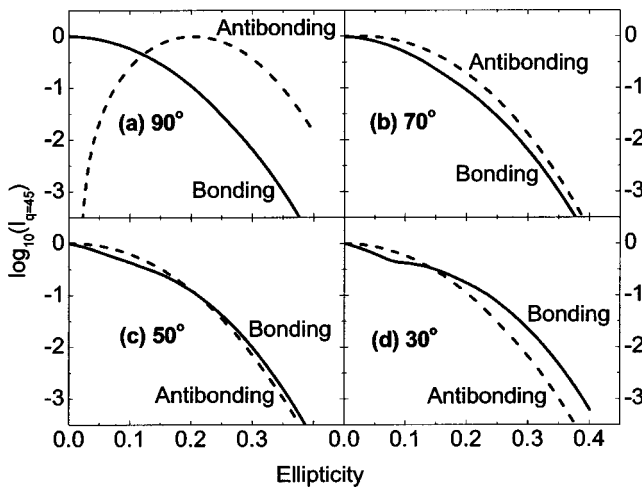


FIG. 3. Calculated ellipticity dependence for the 45th order harmonic from bonding and antibonding molecules with different orientations. Θ is defined as the angle between the molecular axis and the major axis of the ellipse of the electric field. (a) $\Theta = 90^\circ$; (b) $\Theta = 70^\circ$; (c) $\Theta = 50^\circ$; (d) $\Theta = 30^\circ$.

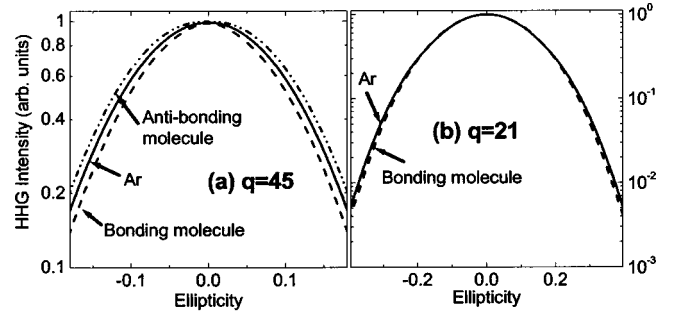


FIG. 4. Calculated ellipticity dependence for (a) 45th and (b) 21st order harmonic from a bonding molecule, an antibonding molecule, and an atom.

order was much weaker than the 21st order, the dynamic range was only about one order of magnitude in this case. For this order, the harmonic signal intensity from O₂ gas drops slower with increasing laser ellipticity than N₂ gas, and that of Ar gas is in between.

To understand the ellipticity dependence difference for N₂ and O₂, we extended the well known Lewenstein model to simulate the harmonic generation from *molecules*. Lewenstein *et al.* have developed an analytical quantum theory to describe high order harmonic generation from *atoms* [19]. The model can be considered as the quantum treatment of the three-step semiclassical model, i.e., the electron first tunnels out of the field-suppressed barrier of the atom, then the freed electron is accelerated by the laser field, finally it recombines with the parent ion and emits a photon. Since our measurement indicated that the molecular high harmonic signal was from the recollision, the model should be valid.

In the Lewenstein model, the harmonic spectrum is calculated from the dipole moment of an atom in the time domain,

$$\vec{x}(t) = i \int_0^\infty d\tau \left(\frac{\pi}{\varepsilon + i\tau/2} \right)^{3/2} \vec{d}^*[\vec{p}_s(t) - \vec{A}(t)] e^{-iS(\vec{p}_s, t, \tau)} \times \vec{E}(t - \tau) \vec{d}[\vec{p}_s(t - \tau) - \vec{A}(t - \tau)] + \text{c.c.}, \quad (1)$$

where ε is a small number, $\vec{p}_s(t, \tau) = \int_{t-\tau}^t dt' \vec{A}(t')$ is the canonical momentum corresponds to the stationary phase. $\vec{A}(t)$ and $\vec{E}(t)$ are the vector potential and the electric field of the laser field. $S(\vec{p}, t, t')$ is the quasiclassical action of the electron moving in the laser field. I_p is the ionization potential of the atom. Finally $\vec{d}[\vec{p}_s - \vec{A}(t)]$ is the field-free dipole transition matrix element between the ground state and the continuum state, under the approximation of the model [20],

$$\vec{d}(\vec{p}) = i \frac{2\vec{p}}{(\vec{p}^2 + \alpha)} \tilde{\phi}(\vec{p}), \quad (2)$$

where $\alpha = 2I_p$, and $\tilde{\phi}(\vec{p})$ is the momentum space wave function for the ground state of the atom. For the 1s state,

$$\vec{d}_{1s}(\vec{p}) = i \frac{2^{7/2}}{\pi} \alpha^{5/4} \frac{\vec{p}}{(\vec{p}^2 + \alpha)^3}. \quad (3)$$

This expression has been used to calculate the ellipticity dependence of harmonic yield for neon atom although its ground state is a $2p$ state, not a $1s$ state [12].

The dipole transition matrix elements for molecules were calculated using Eq. (2), in which the momentum wave functions of the molecules were obtained by following the procedure taken by Lein [21]. Instead of using the exact expression of the wave function in momentum space for O_2 and N_2 , simulation was done for two model diatomic, homonuclear molecules. The two model molecules are only different in that one is a bonding orbital and the other is an antibonding orbital. The wave functions of the molecular orbitals of the model were described as linear combinations of $1s$ atomic orbitals. The LCAO molecular wave functions in the configuration space for bonding and antibonding orbitals are

$$\psi_b(\vec{r}) = \beta[\phi_{1s}(\vec{r}-\vec{R}_1) + \phi_{1s}(\vec{r}-\vec{R}_2)], \quad (4)$$

$$\psi_a(\vec{r}) = \gamma[\phi_{1s}(\vec{r}-\vec{R}_1) - \phi_{1s}(\vec{r}-\vec{R}_2)], \quad (5)$$

respectively, where β and γ are normalization factors. $\vec{R}_1, \vec{R}_2 = \vec{R}_1 + \vec{R}$ are the positions of the nuclei. $|\vec{R}|$ is the equilibrium internuclear separation. The wave function of the $1s$ atomic orbital that forms the molecules is [18]

$$\phi_{1s}(\vec{r}) = \frac{1}{\pi^{1/2} r_0^{3/2}} e^{-r/r_0}, \quad (6)$$

where $r_0 = 1/\sqrt{\alpha}$ is the size of the atom. We took $I_p = 15.8$ eV that equals the binding energy of Ar. The internuclear distance is taken as $\vec{R} = 2\vec{r}_0$. Thus, the atom size is ~ 1 a.u. and the internuclear distance is ~ 2 a.u. The internuclear distance is close to the real values of N_2 (1.098 Å) and O_2 (1.208 Å).

By the Fourier transforms of $\psi_b(\vec{r})$ and $\psi_a(\vec{r})$, the wave functions of the molecular orbitals in the momentum space are

$$\tilde{\psi}_b(\vec{p}) = 2\beta\tilde{\phi}_{1s}(\vec{p})\cos(\vec{p}\cdot\vec{R}/2), \quad (7)$$

$$\tilde{\psi}_a(\vec{p}) = i2\gamma\tilde{\phi}_{1s}(\vec{p})\sin(\vec{p}\cdot\vec{R}/2) \quad (8)$$

and hence the dipole transition matrix element are

$$\vec{d}_b(\vec{p}) = i2\beta\vec{d}_{1s}(\vec{p})\cos(\vec{p}\cdot\vec{R}/2), \quad (9)$$

$$\vec{d}_a(\vec{p}) = 2\gamma\vec{d}_{1s}(\vec{p})\sin(\vec{p}\cdot\vec{R}/2) \quad (10)$$

for a bonding and an antibonding molecule, respectively, where the atomic wave function, $\tilde{\phi}_{1s}(\vec{p})$, in momentum space is the Fourier transform of Eq. (6) and $\vec{d}_{1s}(\vec{p})$ is given by Eq. (3).

The following simulation results were done by inserting Eq. (9) or (10) into Eq. (1). Equations (9) and (10) explicitly show the difference between harmonic generations from molecules than that from atoms. The dipole transition matrices are the product of two terms. The first term is the atomic counterpart and the second term is the interference between the two atomic wave functions in configuration space, simi-

lar to Young's double slit interference in optics. The effect of the interference on the ionization suppression of molecules was considered by Muth-Bohm *et al.* [22].

In the experiment, the molecules in the interaction region were randomly oriented. The measured high harmonic signal was the coherent superposition of the radiation from all the molecules. In the simulation, the ellipticity dependence of the harmonic signal on the orientation angles of the molecules was examined for the 45th order. The orientation angle Θ was defined as the angle between the molecular axis and the major axis of the ellipse of the electric field. The simulation results for $\Theta = 30^\circ, 50^\circ, 70^\circ, 90^\circ$ are shown in Fig. 3. For angles less than 10° , the calculation shows that the HHG signal intensity from bonding molecules decreases slower than from antibonding molecules; however, the difference is small. For angles between 30° and 50° , the HHG signal from antibonding molecules decreases slower than the bonding molecule at small ellipticities, but falls off faster at large ellipticities. For angles larger than 60° , the antibonding molecules show slower decrease for the calculated ellipticity range, in addition, the difference is significant.

For the $\Theta = 90^\circ$ molecule, the simulation results can be explained with a semi-classical theory. The ellipticity dependence for antibonding molecules has been given by Lein [21]. He pointed out that for an antibonding molecule with its axis oriented perpendicular to the electric field of linearly polarized light, the field does not break the *mirror symmetry* of the system, therefore, the momentum space wave function of the molecule in the laser field has a distribution similar to the field free one, as shown in Eq. (8). In other words, the electron tunnels out with a certain initial transverse velocity due to the *sine* term of the wave function, i.e., $\sin(\vec{p}\cdot\vec{R}/2) = 0$ for $\vec{p}\perp\vec{R}$. For a linearly polarized laser pulse, the electron will drift away transversely from the parent ions. This results in a very small recombination probability for the recollision process. With an appropriate amount of ellipticity, the vertical component of the electric field compensates the effect of the transverse initial velocity and drives the drifting electron back to the parent ion, thus enhancing the recombination probability. A similar argument was made to explain the double-ionization of molecules [23].

The argument was extended to bonding molecules. For a bonding molecule with its axis oriented perpendicular to the electric field of a linear light, the field does not change the *symmetry* of the system. This indicates that the initial velocity distribution of the tunneled out electron also has the cosine term, i.e., the probability of an electron tunneling out with its initial velocity along the electric field is larger than in any other direction [$\cos(\vec{p}\cdot\vec{R}/2) = 1$ for $\vec{p}\perp\vec{R}$], as shown in Eq. (7). In this case, when the electric field drives the electron back to the parent ion, the recombination probability is highest for a linearly polarized light pulse. Since the high harmonic originated from radiative recombination of the recollision electron with the parent ion, the harmonic signal will initially increase with the increase of ellipticity for the antibonding molecule. For a bonding molecule, the harmonic signal decreases monotonically. This explains the difference in ellipticity dependence between an antibonding molecule

and a bonding molecule oriented at $\Theta = 90^\circ$. The argument can be extended to other orientation angles.

Figure 4(a) shows the simulation results for the 45th order that summed up the contributions from molecules with random orientation angles. The ellipticity dependence difference between bonding and antibonding molecules still exists, however, the difference is not as large as in the 90° case, because smaller angles yield a smaller the difference. It is worth noting that, for a fixed orientation angle interval, $d\Theta$, the angle dependent weighting factor is proportional to $\sin(\Theta)$. This is because the large angle molecules occupy a larger solid angle for the same $d\Theta$, i.e., $d\Omega = 2\pi \sin \Theta d\Theta$. An approximation is made in the calculation, which assumes that molecules with the same orientation angle make the same contribution regardless of whether they are in the polarization plane or not. The simulation is consistent with our experimentally measured results [Fig. 2(b)]. The simulation results for the 21st harmonic from N_2 and Ar are shown in Fig. 4(b). The difference is very small, which is what was observed in the experiments as shown in Fig. 2(a), but differs from the results of [15].

In conclusion, our experiments showed that for a near

cutoff harmonic, the signal of O_2 molecules falls off slower than Ar and N_2 gas. Our simulations using the Lewenstein model agreed qualitatively with the measured results. To the best of our knowledge, this is the first time that the Lewenstein model and LCAO are combined to simulate harmonic generation from molecules. The model can be refined by using more precise LCAO orbitals; however it is surprising to see that simulation using such simple model molecules recovers the experimental finding. Apart from explaining the experiments, our approach revealed that the field-free dipole transition matrix elements of molecules are orientation dependent, which is an important conclusion for understanding harmonic generation from molecules.

This work is supported by the Division of Chemical Sciences, Office of Basic Energy Sciences, U.S. Department of Energy. The authors acknowledge Dr. Chun Wang for assistance on operating the *Kansas Light Source*. We also thank Dr. Philip Heimann at Lawrence Berkeley National Laboratory for loaning us the x-ray spectrometer. The *Kansas Light Source* was built partially with the support of a MRI grant from the National Science Foundation to Dr. C. L. Cocke and Dr. B. DePaola.

-
- [1] P. Salieres, A. L'Huillier, Ph. Antoine, and M. Lewenstein, *Adv. At., Mol., Opt. Phys.* **41**, 83 (1999).
- [2] T. Brabec and F. Krausz, *Rev. Mod. Phys.* **72**, 545 (2000).
- [3] A. L'Huillier, D. Descamps, A. Johansson, J. Norin, J. Maurisson, and C.-G. Wahlstrom, *Eur. Phys. J. D* **26**, 91 (2003).
- [4] Y. Liang, S. Augst, S. L. Chin, Y. Beaudoin, and M. Chaker, *J. Phys. B* **27**, 5119 (1994).
- [5] C. Lynga, A. L'Huillier, and C. G. Wahlstrom, *J. Phys. B* **29**, 3293 (1996).
- [6] M. Yu. Ivanov and P. B. Corkum, *Phys. Rev. A* **48**, 580 (1993).
- [7] R. Kopold, W. Becker, and M. Kleber, *Phys. Rev. A* **58**, 4022 (1998).
- [8] B. Shan, X. Tong, Z. Zhao, Z. Chang, and C. D. Lin, *Phys. Rev. A* **66**, 061401(R) (2002).
- [9] A. Talebpour, C. Y. Chien, and S. L. Chin, *J. Phys. B* **29**, L677 (1996).
- [10] C. Guo, M. Li, J. P. Nibarger, and G. N. Gibson, *Phys. Rev. A* **58**, R4271 (1998).
- [11] M. J. DeWitt, E. Wells, and R. R. Jones, *Phys. Rev. Lett.* **87**, 153001 (2001).
- [12] P. Antoine, A. L'Huillier, M. Lewenstein, P. Salieres, and B. Carre, *Phys. Rev. A* **53**, 1725 (1996).
- [13] P. B. Corkum, N. H. Burnett, and M. Y. Ivanov, *Opt. Lett.* **19**, 1870 (1994).
- [14] M. Ivanov, P. B. Corkum, T. Zuo, and A. Bandrauk, *Phys. Rev. Lett.* **74**, 2933 (1995).
- [15] A. Flettner, J. Konig, M. B. Mason, T. Pfeifer, U. Weichmann, R. Duren, and G. Gerber, *Eur. Phys. J. D* **21**, 115 (2002).
- [16] B. Shan and Z. Chang, *Phys. Rev. A* **65**, 011804(R) (2002).
- [17] P. B. Corkum, *Phys. Rev. Lett.* **71**, 1999 (1993).
- [18] K. C. Kulander *et al.*, in *Super-Intense Laser-Atom Physics*, Vol. 316 of *NATO Advanced Study Institute, Series B: Physics* (Plenum, New York, 1993), p. 95.
- [19] M. Lewenstein, P. Balcou, M. Y. Ivanov, A. L'Huillier, and P. B. Corkum, *Phys. Rev. A* **49**, 2117 (1994).
- [20] H. A. Bethe and E. E. Salpeter, *Quantum Mechanics of One and Two Electron Atoms* (Academic, New York, 1957).
- [21] M. Lein, *J. Phys. B* **36**, L155 (2003).
- [22] J. Muth-Bohm, A. Becker, and F. H. M. Faisal, *Phys. Rev. Lett.* **85**, 2280 (2000).
- [23] V. R. Bhardwaj, D. M. Rayner, D. M. Villeneuve, and P. B. Corkum, *Phys. Rev. Lett.* **87**, 253003 (2001).